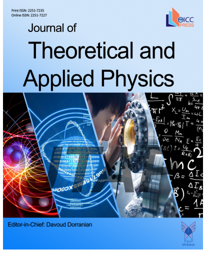

Volume 18, Issue 6, 182484 (1-12)

Journal of Theoretical and Applied Physics (JTAP)

https://dx.doi.org/10.57647/j.jtap.2024.1806.84

A parametric study on coherent wake emission generation based on relativistic laser plasma interaction

Mohammad Nasir Rostami Ravari[1], Alireza Ganjovi[2,*]

[1]*Photonics Department, Sciences and Modern Technologies Faculty, Graduate University of Advanced Technology, Kerman, Iran.*
[2]*Laser Research Department, Institute of Science and High Technology and Environmental Science, Graduate University of Advanced Technology, Kerman, Iran.*

*****Corresponding author:** ganjovi@kgut.ac.ir

Original Research

Received:
10 September 2024
Revised:
5 November 2024
Accepted:
23 November 2024
Published online:
30 December 2024

Abstract:
In this work, a 2D Particle-In-Cell-Monte Carlo Collision (PIC-MCC) simulation scheme is used to study the generation of Coherent Wake Emission (CWE) in the process of attosecond pulse generation based on relativistic laser-plasma interactions. This study uniquely contributes to the field by systematically examining the effects of laser pulse intensity, duration, wavelength, and beam waist which are known as the key operating parameters of incident laser for CWE generation in the process of laser-plasma interactions. The specific conditions that maximize the generated CWE fields are identified to confirm the parameter interactions and threshold values that are critical for efficient CWE generation. It is shown that, under optimal conditions, the CWE field magnitude is maximized at a laser intensity of 3×10^{19} $\mathrm{W/cm^2}$, with further enhancement at a pulse duration of 10^{-13} s and a beam waist size of 5×10^{-5} m. Additionally, both CWE electric and magnetic fields reach peak values at a wavelength of 10^{-5} m. Besides, the threshold values for CWE electric and magnetic fields in the relativistic region were identified at laser intensities of 10^{16} $\mathrm{W/cm^2}$ and 10^{12} $\mathrm{W/cm^2}$, respectively, which are achieved with beam waists of 1.5×10^{-7} m and pulse durations of 5×10^{-16} s. Furthermore, results are compared with existing findings in the literature.

Keywords: Attosecond pulse generation; Coherent wake emission; PIC-MCC simulation scheme

1. Introduction

Nowadays, the attosecond pulses are used for understanding the fundamental nature of different matters. On the other hand, CWE is known as an efficient and confident procedure to generate attosecond pulses. The created attosecond pulses by CWE are normally increased at the higher incident laser intensities. Moreover, the operation of incident laser can be controlled by varying their operational characteristics such as frequency, pulse shape, etc. [1–4]. On the other hand, in the High Harmonic Generation (HHG) process, an intense laser beam interacts with a plasma medium. Hence, the harmonics of the laser frequency will be produced which are multiples of the original photon energy. Notably, CWE is a mechanism for HHG based on the laser beam reflection from an over-dense plasma medium. Besides, the plasma density must exceed the critical density for the corresponding laser wavelength. Furthermore, CWE is a specific type of HHG occurring in over-dense plasma media.

Initially, Cherenkov [5] discovered that when charged particles travel through a medium at speeds faster than the speed of light in that medium, they emit a faint blue glow known as Cherenkov radiation. This phenomenon is a precursor to CWE and provides insights into the behavior of charged particles traveling at high speeds. Moreover, the theoretical framework for CWE began to take shape in the 1970s and 1980s as physicists explored the interactions of charged particles with electromagnetic fields in plasmas and other media. Researchers such as John Dawson [6] made significant contributions to this field. While these studies created a new horizon for emissions, Dromey et al. has recently studied the first narrow band generation of harmonics during the interactions of intense laser pulses with the solid targets such as highly polished fused silica. It was shown that these enhanced generations can provide the basis for a novel and tunable source of coherent wake XUV emission. Besides, it can be used as a powerful tool for the ultrafast plasma diagnostics [1].

Using the high repetition rate laser pulses (mJ level) at the relativistic intensities, Easter et al. studied the characterization of high-order harmonics emission based on the CWE generation procedure. Their experimental structure was including a gold-coated paraboloidal mirror, fused silica target, an iridium-coated diffraction grating, an aluminum filter, and a phosphor-backed microchannel plate as target. Moreover, the experimental findings were compared with 2D- and 3D-PIC simulations. It was found that the FWHM of harmonics divergence was less than 4° when the intensity was maximized. Moreover, it was higher as the laser pulse power was reduced and defocused [3].

Ma et al. used the PIC simulations scheme to study the attosecond pulse generation based on the interactions of relativistic laser pulses with plasma and glass targets. The influences of different parameters, such as laser pulse duration, carrier-envelope phase, and plasma scale length on the significant increasing of the attosecond pulse energy were studied [4].

In a numerical work by Quere et al., a new mechanism was presented for the CWE generation in the interaction of a laser beam with the over-dense plasma media of a fused silica target. It was shown that the transient phase matching between the electromagnetic field and plasma oscillations will lead to the emission of harmonics up to the plasma frequency. It must be noted that these plasma oscillations are periodically excited in the wake of attosecond electron bunches sweeping across the plasma density gradient. Hence, a train of unevenly spaced chirped attosecond pulses will be formed. Furthermore, its direct consequences on the appearance of broadened and chirped harmonics are confirmed experimentally [2].

Andonian et al. [7] reported an experiment demonstrating the CWE generation of in the THz range by a relativistic electron beam in a dielectric-lined slab-symmetric waveguide. The authors show that by using a beam with a bifurcated longitudinal distribution, they can create a driver-witness beam pair, allowing them to observe the wakefield acceleration of the high-energy tail of the beam by about 150 keV in a 2 cm-long DLW. However, CWE involves the emission of coherent Cherenkov radiation from the wakefield excited by the electron beam in the DLW. The authors also characterize the DLW structure through spectral analysis of the CCR from a single electron bunch and from a bunch train with spacing tuned to the second longitudinal mode (TM_{02}) of the DLW. The article claims that this experiment is the first evidence of wakefield acceleration in a dielectric-lined slab-symmetric structure, with potential applications in high-gradient acceleration and narrow-band THz generation.

Lavocat-Dubuis et al. [8] generated the high-order harmonics in the extreme ultraviolet (XUV) range by the reflection of a high intensity femtosecond relativistic laser pulse from a grating of sub-wavelength periodicity. The harmonics production by the CWE process was observed which is the emission from the wakefield excited by the electron bunches that are generated by the laser-grating interaction. Besides, it was found that the CWE signal can be enhanced and tuned by changing the incidence angle, the grating period, and the plasma density. In addition, Liu et al. [9], showed that the intensity of XUV and X-rays does not follow a power law or exponential dependence on frequency, unlike the high harmonic spikes generated through the CWE generation processes.

In an experimental work by Nam et al. [10], the generation of nearly single-cycle pulses with increased intensity and strongly asymmetric pulses of petawatt level by the reflection of a relativistic laser pulse from a thin plasma layer was shown. It was found that, the transmitted pulses have a duration of about 4 fs (1.2 laser cycles) or one-cycle front (tail) asymmetric pulses with peak intensity of about 10^{21} W/cm^2. They also show that the peak amplitude of the transmitted pulse becomes larger than that of the incoming pulse, and intense harmonics are generated. They use particle-in-cell simulations and the analytical flying mirror model to explain the results.

So far, many theoretical and experimental efforts have been performed to understand different features and characteristics of CWE generation in the relativistic laser-plasma interactions. However, a parametric study via consideration of different laser parameters such as laser intensity, wavelength, pulse duration and beam waist in a wide operational range of laser pulses to provide a comprehensive idea on the physical processes in the CWE generation is still absent. Therefore, in this work, the influences of duration, wavelength, and beam waist of incident laser pulses on CWE generation are studied using a 2D PIC-MCC simulation framework. Unlike prior studies, which often focus on the individual laser parameters or specific conditions, this work comprehensively maps out the optimal conditions for CWE generation. Hence, a deeper understanding of how operational parameters impact the formation and characteristics of attosecond pulses will be facilitated. Thus, the obtained results are essential for designing the high-efficiency attosecond pulse generation systems and provides insights into plasma behavior under relativistic laser conditions, which are less explored in this way in the current literature.

2. Simulation model

The developed PIC-MCC algorithm represents a novel simulation scheme that captures the complexities of relativistic laser-plasma interactions in high-temperature and high-pressure Cu vapor environments. This approach advances beyond standard PIC methods by integrating Monte Carlo collision schemes, providing greater accuracy in modeling the influence of multiple operating parameters on CWE generation process. Besides, this refined simulation enables precise adjustments of parameters like laser pulse duration, beam waist, and intensity, which are critical in optimizing CWE fields but they have not been systematically examined under such detailed parametric conditions in previous studies.

The proposed PIC-MCC algorithm simulates the effects of laser electric field on the ionization of neutral gas, the

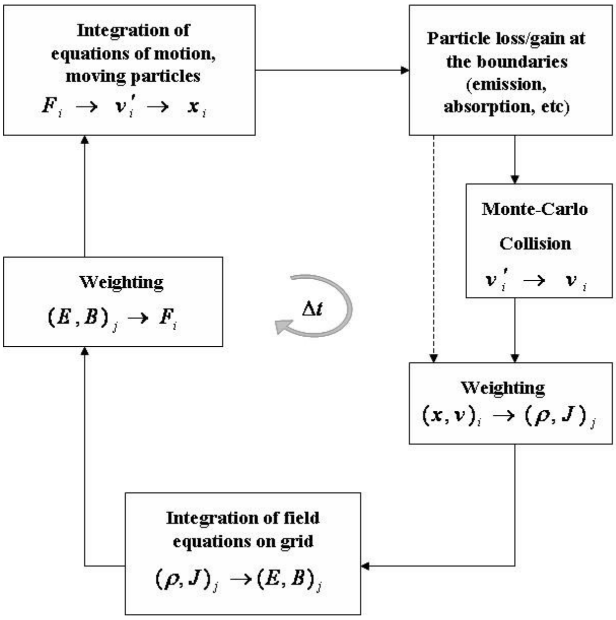

Figure 1. Schematic representation of the computation sequence for Particle in Cell-Monte Carlo Collisions (PIC-MCC) method.

formation and acceleration of the plasma column, and the motion of the charged particles, as shown in Figure 1. The laser field force changes the speed of the charged species as the laser pulse travels through the plasma medium [11]. On the other hand, since the generation of CWE is a complex process, it involves multiple factors. For instance, while electrons are accelerated by the excited medium in high-pressure gases, the CWE field is generated by the acceleration of electrons around the laser beam [12]. Additionally, in an ionized plasma, there are ions present that can be considered "parent ions" to the electrons in the context of their original atomic structure. The interactions between the free electrons and these ions can lead to various phenomena, including the generation of high harmonics [13].
To perform the numerical computations, the scheme needs the potentials and fields in the plasma medium. Hence, they are obtained using Poisson's equation:

$$\nabla \cdot \varepsilon_0 \nabla \Phi(x,t) = \rho(x,t) \tag{1}$$

The potential (Φ) splits as follows:

$$\Phi = \Phi_P + \sum_{\text{Boundaries}} \Phi_L \tag{2}$$

The electrical potential (Φ) has two components: Φ_P, which is due to the Poisson effect, and Φ_L, which is due to the Laplacian effect. The field can be expressed by combining these equations:

$$\nabla \cdot \varepsilon_0 \nabla \Phi_P = -\rho \tag{3}$$

$$\nabla \cdot \varepsilon_0 \nabla \Phi_{Li} = 0 \tag{4}$$

The Poisson field is only caused by the charge in the medium, so the boundary condition for Equation (3) is $\Phi = 0$ on all the boundaries. For each boundary with a fixed potential, the Equation (4) is solved with $\Phi_i = 0$ on the boundary and $\Phi = 0$ everywhere else. This gives us Φ_{Li}, which is the potential from the i^{th} Laplacian field. Φ_L is obtained by adding up all the Laplacian fields. Moreover, the condition that Φ_P is zero for boundaries with a normal derivative is included [14].
One way to preserve energy in the CWE field simulation is to choose the right method and model. The PIC method is a popular choice, but it needs to minimize or fix numerical errors and instabilities. Some methods that can assist with energy preservation in PIC simulations are charge-preserving algorithms, implicit methods, and lattice QED methods. XOOPIC can model various plasma phenomena, such as plasma wakefield acceleration, plasma waves, and some plasma instabilities. It can also reduce some instabilities by limiting inputs.
The interaction between the charged particles and fields can be modeled using the PIC scheme to track the plasma particles in a continuous space and calculates fields on a grid [15]. XOOPIC is a C++ code that uses the PIC scheme in an object-oriented way. It can handle different applications and geometries such as electrostatic and electromagnetic models, The numerical errors and instabilities are minimized or corrected in this XOOPIC programming code [16]. Here, a parallelized XOOPIC code is developed to produce the polarized Gaussian electromagnetic pulses in a high-pressure plasma medium. This modification greatly enhances the running speed of XOOPIC code.
The single laser pulses with ultra-high intensities ($> 10^{12}$ W/cm^2) and pulse durations of less than 1 ps are generally used to irradiate a dense plasma medium for CWE generation. This creates an Electron Plasma Wave (EPW) that follows the incident laser pulse. The EM field oscillates rapidly and forms a plasma wake. The formed wakefield amplitude is the highest when the laser pulse length (L) is about the same as the plasma wavelength, λ_p, where $\lambda_p = 2\pi c/\omega_p$ [17]. This work aims to obtain the variations of CWE field. To this end, the following equations are used to calculate the CWE field inside the plasma medium [18]:

$$\phi(x,t) = \frac{1}{4\pi\varepsilon_0}\int d^3\acute{x}\frac{1}{R}[\rho(\acute{x},\acute{t})]_{ret} \tag{5}$$

$$\mathbf{A}(x,t) = \frac{\mu_0}{4\pi}\int d^3\acute{x}\frac{1}{R}[\mathbf{J}(\acute{x},\acute{t})]_{ret} \tag{6}$$

where $\mathbf{R} = x - \acute{x}$ (Bold characters are vectors) with $R = |x - \acute{x}|$ and $\hat{R} = \mathbf{R}/R$. According to the performed calculations by Lorenz et al. [19], Equations (5) and (6) are used to obtain the electric and magnetic fields. Besides, instead of the wave equations, the Maxwell equations can be used directly. Besides, the fields definitions in terms of the potentials must be implemented. Then, the wave equations for the fields in free space with given charge and current densities can be obtained as follows:

$$\nabla^2\mathbf{E} - \frac{1}{C^2}\frac{\partial^2\mathbf{E}}{\partial t^2} = -\frac{1}{\varepsilon_0}(-\nabla\rho - \frac{1}{C^2}\frac{\partial \mathbf{J}}{\partial t}) \tag{7}$$

The preliminary form of the electric field is:

$$\mathbf{E}(\mathbf{x},t) = \frac{1}{4\pi\varepsilon_0}\int d^3\acute{x}\frac{1}{R}\left[-\acute{\nabla}\rho - \frac{1}{C^2}\frac{\partial \mathbf{J}}{\partial \acute{t}}\right]_{ret} \tag{8}$$

This can be transformed into a more explicit form showing the static limits and the corrections. More specifically, the following expressions can be derived:

$$[\acute{\nabla}\rho]_{ret} = \acute{\nabla}[\rho]_{ret} - \left[\frac{\partial \rho}{\partial \acute{t}}\right]_{ret} \acute{\nabla}(t - \frac{R}{C}) = \acute{\nabla}[\rho]_{ret} - \frac{\hat{\mathbf{R}}}{C}\left[\frac{\partial \rho}{\partial \acute{t}}\right]_{ret} \quad (9)$$

and

$$\begin{aligned}[\acute{\nabla} \times \mathbf{J}]_{ret} &= \acute{\nabla} \times [\mathbf{J}]_{ret} + \left[\frac{\partial \mathbf{J}}{\partial \acute{t}}\right]_{ret} \times \acute{\nabla}(t - \frac{R}{C}) \\ &= \acute{\nabla} \times [\mathbf{J}]_{ret} + \frac{1}{C}\left[\frac{\partial \mathbf{J}}{\partial \acute{t}}\right]_{ret} \times \hat{\mathbf{R}}\end{aligned} \quad (10)$$

Using these expressions in the preliminary solutions and integrating by parts on the first term in each case, the Heaviside-Feynman Expressions for Fields of Point Charge are obtained:

$$\begin{aligned}\mathbf{E}(\mathbf{x},t) &= \frac{1}{4\pi\varepsilon_0}\int d^3\acute{x} \\ &\left\{\frac{\hat{\mathbf{R}}}{R^2}[\rho(\acute{\mathbf{x}},\acute{t})] + \frac{\hat{\mathbf{R}}}{CR}\left[\frac{\partial \rho(\acute{\mathbf{x}},\acute{t})}{\partial \acute{t}}\right] - \frac{1}{C^2 R}\left[\frac{\partial \mathbf{J}(\acute{\mathbf{x}},\acute{t})}{\partial \acute{t}}\right]\right\}\end{aligned} \quad (11)$$

$$\mathbf{B}(\mathbf{x},t) = -\frac{\mu_0}{4\pi}\int d^3\acute{x}\left\{\frac{\hat{\mathbf{R}}}{R^2}[\mathbf{J}(\acute{\mathbf{x}},\acute{t})] + \frac{\hat{\mathbf{R}}}{CR}\left[\frac{\partial \mathbf{J}(\acute{\mathbf{x}},\acute{t})}{\partial \acute{t}}\right]\right. \quad (12)$$

Equations (11) and (12) are also known as Jefimenko's generalizations of the Coulomb and Biot-Savart laws, or Jefimenko's equations [20]. While Jefimenko's fields (JF) alone is incapable of providing a comprehensive solution for calculating CWE fields in all cases, they are important for understanding CWE and its variations. Additionally, variations of CWE can be explored by modifying laser properties within a PIC-MCC simulation framework. Furthermore, while the energy of left and right hand circularly polarized waves of plasma are calculated, the electric and magnetic fields from the spatial gradient of density and plasma waves are added to accurate electric and magnetic fields.
It is worth mentioning that the laser-plasma interaction depends on a dimensionless parameter a_0, often referred to as the normalized laser amplitude. A laser pulse with a normalized amplitude of $a_0 \geq 1$ induces relativistic electron motion. The electron density cut-off for a pulse with $a_o \ll 1$ occurs at a critical density. Additionally, the optimal condition for generating relativistic electrons is ($a_0 > 1$ and $n_e < n_c$) [21]. In this work, the optimal region for relativistic electron generation, along with the condition $a_0 > 1$, is taken into account. Moreover, Cu vapor is considered as the background gas at the atmospheric pressures (about 1 atm) and high temperatures (about 1 eV), and, all the results are for a specific plasma, which will be mentioned in the following.

3. Simulation results and discussions

The obtained results confirm how fine-tuning laser pulse parameters, such as intensity and beam waist, can lead to significant CWE field enhancement, particularly under relativistic conditions. This systematic optimization across a range of intensities and pulse durations allows for unprecedented insights into the thresholds necessary to achieve stable CWE fields for practical attosecond pulse generation. Hence, a novel contribution to the understanding of laser-plasma interaction mechanisms and their practical applications in generating ultra-fast, high-energy pulses is provided.
The threshold values for the electric and magnetic fields in CWE generation process are significant since they can establish the minimum intensities which are required for the observable CWE, particularly under relativistic conditions. These thresholds are essential for understanding the operational window within which CWE can be generated. Specifically, the thresholds indicate the onset of CWE generation, where field intensities are sufficient to induce coherent wake effects without necessarily reaching maximum possible values. This is valuable for experimental setups where achieving maximum intensities may be impractical or costly. Moreover, by identifying the field thresholds, the minimum requirements for generating CWE can be determined and, hence, the experimental designs will be optimized accordingly. Furthermore, this approach allows for a more cost-effective and realistic assessment of operational parameters, as experiments can be planned within feasible intensity ranges rather than aiming for the absolute peak values.
In the performed simulations for CWE generation process using PIC-MCC scheme, a high-intensity laser pulse is used. Besides, the laser pulse is linearly polarized with a transverse Gaussian profile. Moreover, the simulations are performed in a region with the spatial dimensions of L_x (The axis that is parallel to the direction of laser) and L_y (The axis that is perpendicular to the direction of laser) which are divided into $N_x \times N_y$ cells. These values are the initial inputs that are briefly mentioned in Table 1.
These values are the initial inputs that are briefly outlined in Table 1. It must be noted that, they are derived from the various experimental and theoretical studies [2, 12, 22–24]. It is important to note that the simulation parameters, specifically waist size (W_s), pulse duration (P_d), and time step (T_{step}) are selected based on the following physical conditions:
W_L: $W_L <= W_s < L_x$, L_y so, $W_L <= 3.0 \times 10^{-5}$ m, and

Table 1. Initial input parameters.

Parameter	Default value
Peak laser intensity	3×10^{15} W/cm^2
Laser pulse length FWHM	6.7×10^{-15} s
Laser wavelength	1.0×10^{-6} m
Laser waist size	5.0×10^{-6} m
Simulations dimension L_x	3.0×10^{-5} m
Simulations dimension L_y	5.0×10^{-5} m
N_x	2048
N_y	256
Simulations time step	4.1×10^{-17} s
Plasma density	10^{25} m^{-3}
Number of plasma particles per simulation particles	1×10^{10}
Background gas	Cupper
Initial electrons temperature	1 eV

$W_L >$ simulation grids length so, $W_L > 2.8 \times 10^{-8}$ m $*20$ finally, 5.8×10^{-7} m $< W_L <= 5.0 \times 10^{-5}$ m.
P_d: $T_{\text{step}} \ll P_d$ so, 4.1×10^{-17} s $< P_d < 1.31 \times 10^{-1}$ s, and $P_d >= 10 * T_{\text{period}} = 1/\text{Frequency}$ so, 4.8×10^{-16} s $<= P_d$.
W_s: $W_L =< W_s < L_y$ so, 1.5×10^{-7} m $=< W_s < 5.0 \times 10^{-5}$ m.
Physically, while the laser wavelength will not exceed its waist size, they both are independent laser parameters and can be controlled separately. In the performed simulations using the XOOPIC programming code, the simulation length or domain size must be larger than the laser wavelength. Hence, the laser-plasma interactions along with as diffraction, reflection, scattering etc. can be accurately simulated. Therefore, to perform the meaningful and accurate simulations, the simulation length must be at least several times larger than the input laser wavelength. On the other hand, the simulation length in the XOOPIC computations refers to the spatial extent or size of the simulation domain. However, depending on the specific parameters and simulations setup, the laser waist size can be smaller, larger, or even comparable to the simulation length. However, it is suggested to adjust the simulation length to encompass the entire simulation region of interest to ensure the accuracy. Hence, the simulation adequately captures the laser-plasma interactions throughout the desired spatial extent. Moreover, for the laser waist sizes significantly larger than the simulation length, the simulation parameters adjustment or considering a larger simulation domain is necessary to obtain more accurate results. On the other hand, in the numerical simulations using the XOOPIC code, the simulation time-step is a critical parameter and, it may determine the temporal resolution of simulation. In addition, the time-step represents the discrete intervals at which the simulation updates the positions and velocities of particles, fields, etc.
Additionally, the Full Width at Half Maximum (FWHM) of a laser pulse is a measure of the temporal extent of the pulse. To perform the accurate simulations, the simulation time-step must be significantly smaller than the laser FWHM. For the time-steps larger than the FWHM, the simulation might miss the important temporal features of the pulse, leading to unpredicted inaccuracies in the results. Hence, the simulation may inadequately capture some phenomena such as pulse shaping, temporal evolution of plasma dynamics, or other time-dependent processes. Therefore, the simulation time-step must be chosen smaller than the laser FWHM to guarantee the simulation accuracy.
Here, the input laser wavelength is considered smaller than the simulation dimensions. Adams et al. stated that the target should be opaque for the laser to generate the CWE field [25]. Hence, as a target, the plasma medium will be possibly changed from opaque to transparent when the laser frequency is varied. However, these variations depend on the plasma and laser operational parameters. On the other hand, the formula for the critical density is defined as $n_C = m_e \varepsilon_0 \omega^2 / e^2$. Where n_C is the critical density, m_e is the electron mass, ε_0 is the vacuum permittivity, ω is the laser angular frequency, and e is the electron charge [26]. The critical density is equivalent to the maximum plasma density that a laser pulse can penetrate. Hence, while the target is opaque at densities higher than the critical density, it is transparent for the densities below the critical density [26]. Besides, the critical density is directly influenced by the laser frequency. Thus, the laser pulses with higher frequencies can penetrate the denser plasma targets. Therefore, while at the higher laser frequencies, an initially opaque target can be converted to a transparent medium, the lower laser frequencies can make a transparent target opaque.
In this work, the interaction medium has a simple geometry, consisting of a 2D plasma medium with a laser entering this geometry along the axis perpendicular to the y-axis at $x = 0$. Figure 2 (a) illustrates this geometry, depicting an almost homogeneous plasma environment with no interaction with the laser. Figure 2 (b) provides an example of the plasma-laser interaction environment, showing the waves created in the electrons (represented as beige dots) and the spatial gradient of their density.
Based on initial input parameters (Table 1), a wide range for the obtained frequency spectrum of CWE is shown in Figure 3 (a). Figure 3 (a) shows electric and magnetic field of plasma medium and matched harmonics of laser (LH). The FFT (Fast Fourier Transform) function is used to convert the time-domain signals into frequency-domain. The plasma Frequency is calculated using the formula for plasma frequency, and the harmonics are simply multiples of the laser frequency. For a more accurate calculation, the fields resulting from the laser and once again the fields resulting from the plasma without interaction with the laser were measured and subtracted from the fields resulting from the interaction of the laser and plasma ($B = B_{\text{Interaction}} - B_{\text{Laser}}$).
Moreover, as seen in Figure 3 (b), there is an overall reduc-

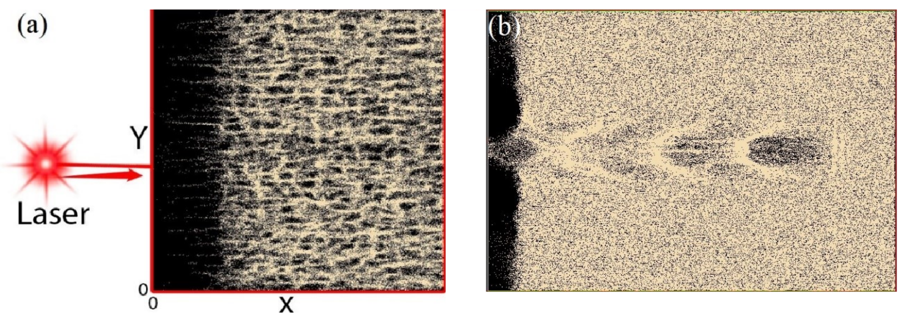

Figure 2. (a) simple 2D interaction geometry with an almost homogeneous plasma environment, (b) an example of the plasma-laser interaction environment

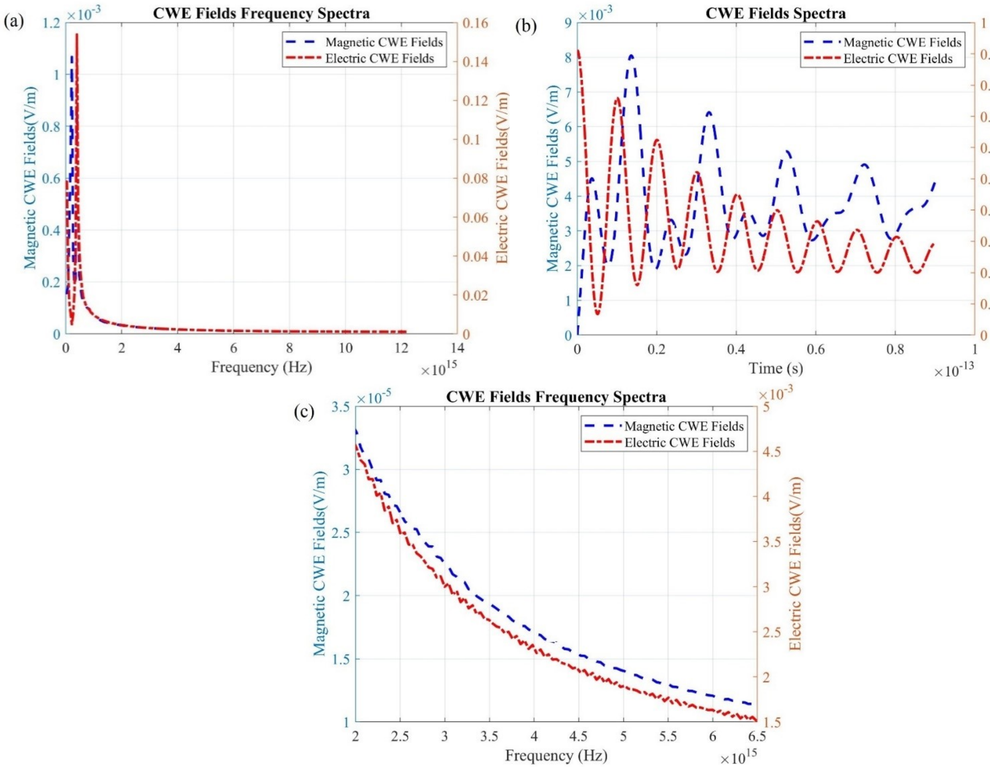

Figure 3. (a) The Fast Fourier Transform (FFT) of generated CWE fields, (b) the temporal variations of the CWE fields, (c) attosecond region of the CWE fields.

tion in the temporal variations of CWE field. The findings by Quéré et al. [2] and Bagnoud et al. [27] confirm the reduction in the temporal variations of CWE field magnitude. Besides, as shown in Figure 3 (c), the pulse width of the formed CWE is in the range of attoseconds.

To determine the optimal parameter values for CWE generation, a systematic simulation approach is employed using a PIC-MCC framework. Here, the key operational parameters of the incident laser pulse i.e., laser intensity, frequency, pulse duration, and beam waist are adjusted in sequential simulations to understand their individual and combined effects on CWE field magnitude. Hence, each simulation began with a baseline set of initial parameters, as outlined in Table 1. Then, one parameter is iteratively modified at a time while holding the others constant to isolate each effects of parameter on CWE generation process. Besides, for each parameter, adjustments are made incrementally until one of three outcomes are observed: a maximum CWE field value, a threshold limit, or a saturation in CWE field values, indicating no further significant impact. Consequently, after identifying the optimal value for a given parameter (e.g., laser intensity), it is set as the new baseline for subsequent simulations of the next parameter. Using this iterative process, a progressively refinement of the parameters is allowed. Hence, the best values from each stage into the next is incorporated which is reflected in a convergence on a set of optimal conditions for CWE field generation. However, this stepwise approach is helpful to identify the parameter settings that maximize the CWE fields and detection of threshold values that differentiate non-relativistic from relativistic effects.

In following, for CWE generation, the laser pulse intensity is initially varied within the range of 10^{12} to 8×10^{21} $\mathrm{W/cm^2}$ to observe the laser intensity effects on the resulting CWE fields.

Moreover, as seen in Figure 4 for the variations of CWE fields versus the input laser intensity, while the CWE electric and magnetic fields threshold are about 4×10^{10} V/m and 10^1 Tesla corresponding to input laser intensity of 1×10^{16} $\mathrm{W/cm^2}$, and 10^{12} $\mathrm{W/cm^2}$, respectively, they are maximized at 2×10^{12} V/m and the laser intensity of 3×10^{19} $\mathrm{W/cm^2}$. As shown, at the laser intensities below 3×10^{19} $\mathrm{W/cm^2}$,

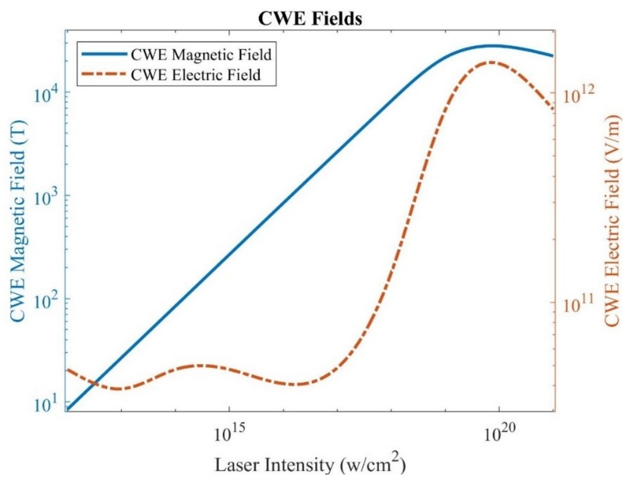

Figure 4. The magnitudes of CWE electric and magnetic fields as a function of the intensity of input laser pulses.

the CWE field increases owing to the transition from its modulated to continuous spectra, its higher repetition rate, and spectral coherence enhancement [28].

In an experimental work, Dromey et al. demonstrated that the very high laser intensities lead to relativistic and nonlinear effects on the plasma medium, with the CWE maximum which was observed at approximately $I \approx 4 \times 10^{19}$ W/cm^2. Their findings were in agreement with the results shown in Figure 4. Additionally, this phenomenon imposes certain limits on harmonic order and the emission energy of CWE, as well as on the quality and stability of attosecond pulses [1]. Furthermore, Kallala et al. [29] confirmed that while the CWE generation process initiates at laser intensities around 10^{16} W/cm^2, relativistic effects become prominent at intensities greater than 10^{18} W/cm^2. Additionally, Golovin et al. [30] verified that using a high-power laser pulse at 10^{19} W/cm^2 can generate a magnetic field on the order of Kilo-Tesla.

The equation for wake-field generation can be expressed as

$$\frac{d^2x}{d\zeta^2} = \frac{1}{2}\left(\frac{1+a^2(\zeta)}{x^2} - 1\right),$$

where $x = 1+\phi$ represents the modified electrostatic potential, and $a^2(\zeta)$ is the dimensionless laser intensity envelope averaged over fast oscillations. In the context of laser-plasma interactions, the plasma response is described in terms of the independent dimensionless variables $\zeta = k_p(z - v_g t)$ and $\tau = k_p ct$ where k_p is the plasma wavenumber, and $v_g \approx -c$ is the laser group velocity (for simplicity, it is assumed that the laser propagates in the negative z direction). Moreover, the normalized wake-field is calculated as $\varepsilon = -dx/d\zeta = eE/mc\omega_p A$. This serves as a formal solution for the electric field. Outside the laser, it can be expressed as $[\varepsilon^{\text{out}}(\zeta)]^2 = -((x-1)^2)/x + \int_{-\infty}^{\infty} a^2(\acute{x}/x^2)d\zeta$. This expression reaches a maximum value given by $[\varepsilon_{\max}^{\text{out}}]^2 = \int_{-\infty}^{\infty} a^2(\zeta)(\partial/\partial\zeta)(1/x)d\zeta$ at $x = 1$ [22]. These equations demonstrate that the wake-field and its maximum depend on the laser intensity; however, this relationship is not linear.

Finally, it is worthy to mention that, when the laser intensity I_0 exceeds 10^{22} W/cm^2, quantum-electrodynamics (QED) processes can happen in laser-matter interactions. QED effects are quantum electrodynamics processes that occur in strong electromagnetic fields, like those from ultra-intense lasers or relativistic beams [31].

It is well-known that, the shorter wavelengths correspond to higher photon energies, allowing lasers to achieve higher intensities by focusing photons on smaller areas. Thus, for the studies on laser-plasma interactions, high intensities are needed for specific applications. Hence, in the performed studies on the laser plasma interactions by many researchers, the high intensity laser pulses are used. For instance, Quéré et al. [2], used high intensity (4×10^{15} W/cm^2) and high frequency (7.49×10^{15} Hz) laser pulses for experimental study in CWE. In addition, Fedeli et al. [32] stated that the optimum frequency depends on the several factors. These factors are mainly including the laser intensity, harmonics generation mechanism, plasma density, and temperature gradients. However, these factors are remained constant in this work.

It must be noted that, to study different features of CWE, it is important to find the optimal frequency of input laser pulses. Hence, as shown in Figure 5, CWE fields are maximized at the wavelength of 1×10^{-5} m. It shows that at the frequencies close to the plasma frequency (1.7×10^{14} Hz $\sim 1.06 \times 10^{-5}$ m), the CWE fields are maximized which is due to electrons resonance. The findings by Kubodera et al. [33] show that, under the resonance conditions, the wave number variations of a single harmonic are important at the harmonic frequencies close to the atomic transition frequency.

In an experimental study, Quéré et al. [2] demonstrated that the transient phase matching between the electromagnetic field and plasma oscillations within a density gradient can drive harmonic generation up to the plasma frequency. This finding supports the idea of a peak CWE response at the plasma frequency of the incident laser. On the other hand, In a comparative study by Malik et al. [34] the analytical expressions were derived for the wake-field which was generated behind a laser pulse propagating in a plasma discharge medium. They demonstrated that both the wake-field and the associated energy gain are enhanced at the higher laser frequencies, supporting the results shown in Figure 5. Another study by Heydarzadeh et al. [35] confirms that the group velocity depends on frequency, described by the equation

$$v_g = c\sqrt{\frac{\omega^2 - \omega\omega_p^2/(\omega-\omega_c)}{\omega + \omega_c\omega_p^2/[2(\omega-\omega_c)^2]}},$$

Hence, given the relationship between CWE and group speed, it follows that laser frequency significantly affects CWE. Furthermore, the normalized equation for the laser wake-field is given by

$$\frac{\partial \tilde{E}_\omega}{\partial \tilde{\zeta}} = \frac{\tilde{\varphi}}{\beta_g^2} - [1 + \frac{\beta_g}{\tilde{\omega}-1}\sqrt{1 - \frac{\tilde{\omega}_p^2}{\tilde{\omega}(\tilde{\omega}-1)}}]\frac{\tilde{\omega}|a|^2}{\beta_g^2(\tilde{\omega}-1)},$$

where the frequency of the laser pulse (ω) and the plasma frequency (ω_p) are normalized by the cyclotron frequency

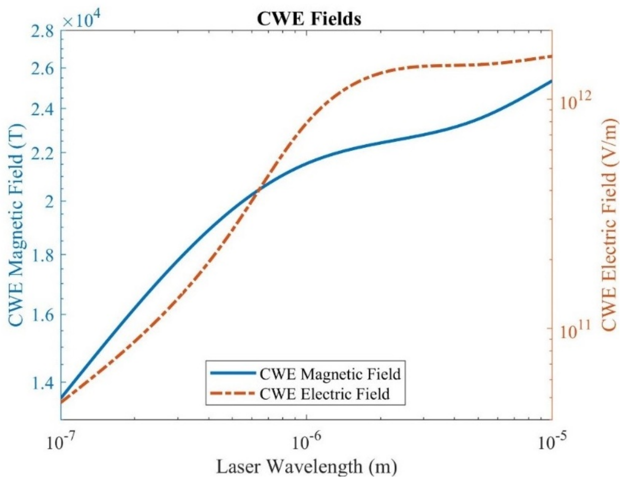

Figure 5. The CWE fields versus the wavelength of input laser pulse.

(ω_c) and $v_g = c\beta_g$. This serves as theoretical support for Figure 5, which illustrates that the laser wake-field depends on the frequency of the laser.

The laser pulse duration is largely independent of its wavelength. This is due to the separation between temporal coherence (pulse duration) and spectral coherence (wavelength). Techniques like mode-locking produce ultra-short pulses unaffected by central wavelength, while dispersion management ensures consistent pulse duration across different applications. For instance, Porat et al. used lasers with a central wavelength of 800 nm and pulse durations in the attosecond range. The study also mentions femtosecond (fs) Ti-Sa lasers, known for short pulse durations, and CO_2 lasers, which typically have longer wavelengths. On the other hand, this is well-known that, at a given input laser intensity, the longer pulse durations will influence the features of CWE generation. According to one article by Tomassini et al. [36], the minimum laser pulse duration for creating attosecond pulses by wakefield is about 30 fs FWHM. When the laser pulse is longer than the plasma period, the laser absorption is strong and, the plasma dispersion is weak. Thus, the CWE fields will grow with the laser pulse duration. The maximum laser pulse duration is approximately equal to the plasma period of $\tau_p = 2\pi(\varepsilon_0 m*/n_e e^2)^{1/2}$ [37].

As shown in Figure 6, both the CWE electric and magnetic fields vary similarly with the laser pulse durations. This might be due to the increasing influences of laser pulse duration on the kinetic energy of electrons. In addition, while CWE fields are maximized at the input laser pulse duration of 10^{-13} s, the thresholds to initiate their variations occur at the duration of 5×10^{-16} s.

Elnasharty et al. [38] showed that, with the longer laser pulses of constant intensity, the electron density increase. Besides, Malik et al. [34] found that both the wake-field and the corresponding energy gain are enhanced with larger pulse durations. These findings support the results presented in Figure 6. Gopal et al. [39] used the skewed laser pulses of optimal pulse length to enhance electron beam generation through laser wake-field acceleration. The optimal laser pulse length for exciting plasma waves in the linear regime ($a_0 < 1$) is calculated as $\tau_L = \lambda_p/\sqrt{2\pi}c$. However, in the nonlinear regime ($a_0 > 1$), the optimal pulse length remains uncertain. For the parameters illustrated in Figure 6, τ_L is determined as $\tau_L = 4.4\times10^{-14}$, which supports the findings presented in Figure 6. Furthermore, Sharma et al. [40] experimentally showed that there is a mutual connection between the laser pulse length and plasma density that must be considered for energy-efficient electron acceleration. Additionally, since CWE generation process is related to spatial and temporal plasma density gradients, it also correlates with electron acceleration. Additionally, Spitkovsky et al. [22] found that the wake excitation by arbitrary laser shapes can be parameterized using pulse length. They showed that the total energy available in the wakefield can be calculated using the equation

$$e_0 = 2k_0 + \frac{\tau_L[k_0^2 + (1-k_0\tau_L)^3}{(1-k_0\tau_L)},$$

where k_0 is a constant related to photon deceleration throughout the pulse, and τ_L is the laser pulse length.

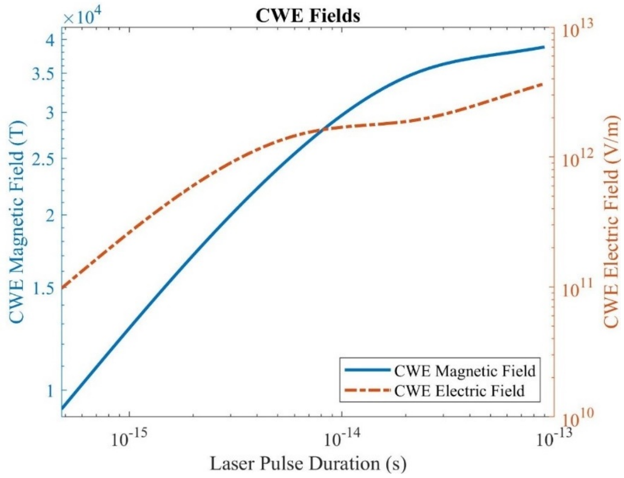

Figure 6. The magnitude of CWE electric and magnetic fields as a function of duration of input laser pulses.

It must be noted that, at a constant wavelength, the laser waist size depends on the beam propagation angle and distance from the laser beam waist. Thus, the laser spot size can be independent of the wavelength. In addition, depending on the laser wavelength, the lowest waist size for a laser beam is limited by the diffraction [41]. As seen in Figure 7, while CWE fields are increased versus the laser pulse waist size, they both get maximized at the waist size 5×10^{-5} m. In this case, the laser affects the entire simulation environment. In such a situation, it is reasonable the CWE fields get maximized. Besides, the mostly linear increasing of radiation at the higher waist sizes seems quite logical.

Existing experimental and theoretical studies show that when the laser beam waist size is comparable to the plasma wavelength, it can lead to the enhanced CWE fields [42, 43]. Conversely, smaller laser pulse waist sizes can result in the reduced CWE fields due to excessive group velocity mismatch and plasma expansion [44, 45]. Furthermore, the reduction in waist size is associated with shorter Rayleigh lengths [12]. Additionally, the thresholds for initiating

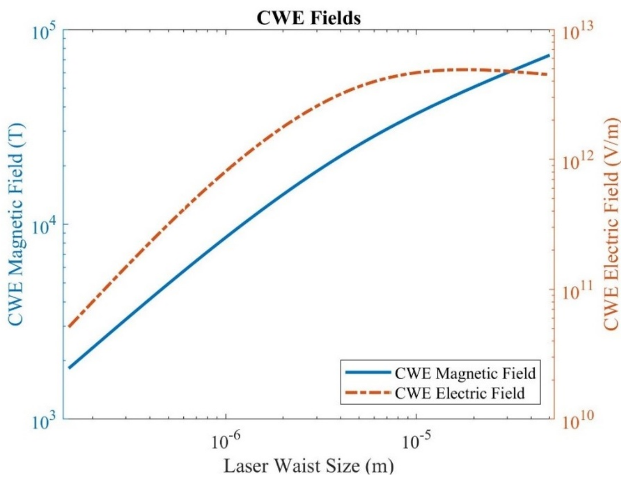

Figure 7. The CWE electric and magnetic fields magnitude versus the beam waist of input laser pulses.

variations in CWE fields are observed at a waist size of 1.5×10^{-7} m.

Based on previous studies [46, 47], the electric field of a laser pulse can be described as:

$$a = a_0 \frac{r_0}{r_s} \times \exp\left[-\frac{y^2}{r_s^2} - \frac{z^2}{r_s^2} - \frac{(t-t_0)^2}{2T_L^2}(1+\frac{b(t-t_0)}{((t-t_0)^2+T_L^2)^{1/2}})^{-1} \right] \times \cos\left(k(x-x_0) - \omega t + \frac{(y^2+z^2)(x-x_0)}{r_s^2 \times Z_R} - \tan^{-1}(\frac{x-x_0}{Z_R}) \right)$$

where $r_s = r_0(1+(x-x_0)^2/Z_R^2)^{1/2}$ is the laser spot size, r_0 is the beam waist, $Z_R = kr_0^2/2$ is the Rayleigh length, x_0 is the focal position, T_L is the pulse duration, t is the simulation time, t_0 is the time when the laser amplitude peaks, and b is the skew parameter ($|b| < 1$), which measures the asymmetry in the pulse shape. This equation establishes the relationship between the laser spot size (or beam waist) and the laser pulse electric field. The electric field of the laser pulse exerts a Lorentz force on the electrons, while the collective behavior of the plasma results in a density gradient. Consequently, this equation demonstrates the complex relationship between the beam waist size and the CWE generation.

In addition, these findings offer the valuable insights for advancing research and development in the applications of attosecond laser technology. By identifying optimal laser parameters such as intensity, pulse duration, wavelength, and beam waist, these results can guide the configuration of laser systems designed to generate attosecond pulses efficiently. The detailed examination of these parameters aids in refining input laser specifications to maximize CWE generation which is a key factor in creating high-quality attosecond pulses. On the other hands, this research will practically provide a foundation for more targeted experiments, potentially lowering operational costs and enhancing output quality. However, the future applications may involve more precise control over attosecond pulse characteristics for use in ultrafast imaging, spectroscopy, and high-field physics. Ultimately, these findings contribute to a deeper understanding of relativistic laser-plasma interactions and inform the engineering of next-generation attosecond technologies.

4. Conclusion

This work provides a novel parametric study that is instrumental in identifying the precise operational thresholds for CWE generation through the laser-plasma interactions, which can directly inform experimental setups and future designs in attosecond pulse generation technologies. By systematically mapping the effects of laser intensity, wavelength, duration, and beam waist in a high-pressure Cu plasma medium, this study bridges the theoretical gaps and aligns with experimental findings. Thus, a foundational framework for advancing high-field, high-precision plasma-based applications is provided. Moreover, it is worth mentioning that many observed trends aligned with existing experimental and theoretical findings. Notably, CWE fields were maximized at laser intensities of approximately 3×10^{19} W/cm^2. In addition, CWE fields peaked at an input laser wavelength of 1×10^{-5} m, but achieved maxima at a pulse duration of 10^{-13} s, with the latter reflecting the energy transfer from the laser to the plasma medium. Besides, at the constant laser intensities, CWE fields were optimized with a laser pulse waist size of 5×10^{-5} m. Furthermore, the thresholds for initiating the variations in CWE electric and magnetic fields in the relativistic region were identified at the laser intensities of 1×10^{16} W/cm^2, and 10^{12} W/cm^2, respectively. They achieved at laser beam waists of 1.5×10^{-7} m, and pulse durations of 5×10^{-16} s. Moreover, minimum values for CWE fields occurred at a laser wavelength of 1.5×10^{-7} m.

Acknowledgements

The authors would like to acknowledge the Institute of Science and High Technology and Environmental Sciences, Graduate University of Advanced Technology for the financial support within the Project No. 2628/99/S/7-27/12/1399.

Authors contributions

The authors have contributed equally to prepare the paper.

Availability of data and materials

The data that support the findings of this study are available from the corresponding author upon reasonable request. Due to the nature of the simulation results and the computational methods used, the raw data and simulation codes are not publicly available but can be shared with qualified researchers for academic purposes.

Conflict of interests

The author declare that they have no known competing financial interests or personal relationships that could have appeared to influence the work reported in this paper.

References

[1] B. Dromey, S. G. Rykovanov, D. Adams, R. Hörlein, Y. Nomura, D. C. Carroll, P. S. Foster, S. Kar, K. Markey, and P. McKenna. "Tunable enhancement of high harmonic emission from laser solid interactions.". *Physical Review Letters*, **102**:225002, 2009. DOI: https://doi.org/10.1103/PhysRevLett.102.225002.

[2] F. Quéré, C. Thaury, P. Monot, S. Dobosz, P. Martin, J.-P. Geindre, and P. Audebert. "Coherent wake emission of high-order harmonics from overdense plasmas. ". *Physical Review Letters*, **96**:125004, 2006. DOI: https://doi.org/10.1103/PhysRevLett.96.125004.

[3] J. H. Easter, J. A. Nees, B. X. Hou, A. Mordovanakis, G. Mourou, A. G. R. Thomas, and K. Krushelnick. "Angular emission and polarization dependence of harmonics from laser–solid interactions. ". *New Journal of Physics*, **15**:025035, 2013. DOI: https://doi.org/10.1088/1367-2630/15/2/025035.

[4] G. Ma, W. Dallari, A. Borot, F. Krausz, W. Yu, G. D. Tsakiris, and L. Veisz. "Intense isolated attosecond pulse generation from relativistic laser plasmas using few-cycle laser pulses. ". *Physics of Plasmas*, **22**:033105, 2015. DOI: https://doi.org/10.1063/1.4914087.

[5] P. A. Cherenkov. "Visible light from clear liquids under the action of gamma radiation. ". *Comptes Rendus (Doklady) de l'Aeademie des Sciences de l'URSS*, **2**: 451–454, 1934.

[6] P. Kaw and J. Dawson. "Relativistic nonlinear propagation of laser beams in cold overdense plasmas.". *The Physics of Fluids*, **13**:472–481, 1970. DOI: https://doi.org/10.1063/1.1692942.

[7] G. Andonian, D. Stratakis, M. Babzien, S. Barber, M. Fedurin, E. Hemsing, K. Kusche, P. Muggli, B. O'Shea, X. Wei, O. Williams, V. Yakimenko, and J. B. Rosenzweig. "Dielectric wakefield acceleration of a relativistic electron beam in a slab-symmetric dielectric lined waveguide. ". *Phys. Rev. Lett.*, **108**:244801, 2012. DOI: https://doi.org/10.1103/PhysRevLett.108.244801.

[8] X. Lavocat-Dubuis and J.-P. Matte. "Numerical and theoretical study of the generation of extreme ultraviolet radiation by relativistic laser interaction with a grating.". *Physics of Plasmas*, **17**:093105, 2010. DOI: https://doi.org/10.1063/1.3485119.

[9] X. Liu, D. Yue, Q. Dong, Z. Shao, Z. Li, H. Teng, Z. Wei, F. Liu, B. Li, X. Yuan, M. Chen, Z. Sheng, and J. Zhang. "Generation of extreme-ultraviolet and x-ray light from a propagating nanometer electron layer in few-cycle laser interaction with solid targets. ". *Phys. Rev. A*, **109**:043519, 2014. DOI: https://doi.org/10.1103/PhysRevA.109.043519.

[10] I. Nam, V. V. Kulagin, M. S. Hur, I. W. Lee, and H. Suk. "Generating nearly single-cycle pulses with increased intensity and strongly asymmetric pulses of petawatt level. ". *Phys. Rev. E*, **85**:026405, 2012. DOI: https://doi.org/10.1103/PhysRevE.85.026405.

[11] M. N. R. RAVARI, A. Ganjovi, F. Shojaei, and A. Falahat. "Temperature measurements in a manufactured RF plasma jet in various Ar/N_2 mixtures. ". *Turkish Journal of Physics*, **41**:507–519, 2017. DOI: https://doi.org/10.3906/fiz-1705-10.

[12] E. Porat, H. Yehuda, I. Cohen, A. Levanon, and I. Pomerantz. "Diffraction-limited coherent wake emission. ". *Physical Review Research*, **3**:L032059, 2021. DOI: https://doi.org/10.1103/PhysRevResearch.3.L032059.

[13] V. E. Fortov, I. T. Iakubov, and A. G. Khrapak. "Electrical conductivity of fully ionized plasma. ". *Physics of Strongly Coupled Plasma*, , 2006. DOI: https://doi.org/10.1093/acprof:oso/9780199299805.003.0007.

[14] A. Barkhordari, A. Ganjovi, I. Mirzaei, A. Falahat, and M. N. Rostami Ravari. "A pulsed plasma jet with the various Ar/N_2 mixtures. ". *Journal of Theoretical and Applied Physics*, **11**:301–312, 2017. DOI: https://doi.org/10.1007/s40094-017-0271-y.

[15] J. P. Verboncoeur. "OOPIC: object oriented particle-in-cell code.". *International Conference on Plasma Science, IEEE*, :244, 1995. DOI: https://doi.org/10.1109/PLASMA.1995.533235.

[16] J. P. Verboncoeur. "Particle simulation of plasmas: review and advances. ". *Plasma Physics and Controlled Fusion*, **47**:A231, 2005. DOI: https://doi.org/10.1088/0741-3335/47/5A/017.

[17] V. V. Strelkov, V. T. Platonenko, A. F. Sterzhantov, and M. Y. Ryabikin. "Attosecond electromagnetic pulses: generation, measurement, and application. Generation of high-order harmonics of an intense laser field for attosecond pulse production. ". *Physics-Uspekhi*, **59**:425, 2016. DOI: https://doi.org/10.3367/ufne.2015.12.037670.

[18] J. D. Jackson. "Classical electrodynamics.". *American Association of Physics Teachers*, 1999.

[19] L. Lorenz. "XXXVIII. On the identity of the vibrations of light with electrical currents. ". *The London, Edinburgh, and Dublin Philosophical Magazine and Journal of Science*, **34**:287–301, 1867. DOI: https://doi.org/10.1080/14786446708639882.

[20] J. Van Bladel. "Lorenz or Lorentz? ". *IEEE Antennas and Propagation Magazine*, **33**:69, 1991. DOI: https://doi.org/10.1109/MAP.1991.5672647.

[21] A. Arefiev, V. Khudik, A. Robinson, G. Shvets, L. Willingale, and M. Schollmeier. "Beyond the ponderomotive limit: Direct laser acceleration of relativistic electrons in sub-critical plasmas.". *Physics of Plasmas*, **23**, 2016. DOI: https://doi.org/10.1063/1.4946024.

[22] A. Spitkovsky and P. Chen. “Laser shaping and optimization of the laser-plasma interaction. ”. *AIP Conference Proceedings*, :183–194, 2001. DOI: https://doi.org/10.1063/1.1384349.

[23] T. Tajima, X. Q. Yan, and T. Ebisuzaki. “Wakefield acceleration. ”. *Rev. Mod. Plasma Phys.*, **4**:7, 2020. DOI: https://doi.org/10.1007/s41614-020-0043-z.

[24] C. Thaury, F. Quere, J.-P. Geindre, A. Levy, T. Ceccotti, P. Monot, M. Bougeard, F. Réau, P. d’Oliveira, and P. Audebert. “Plasma mirrors for ultrahigh-intensity optics. ”. *Nature Physics*, **3**:424–429, 2007. DOI: https://doi.org/10.1038/nphys595.

[25] D. Adams, B. Dromey, M. Geissler, S. Kar, K. Markey, M. Zepf, R. Hörlein, Y. Nomura, S. Rykovanov, G. Tsakiris, et al. “Tunable enhancement of coherent wake emission harmonics from laser solid interactions. ”. *HIGH POWER LASER SCIENCE I Femtosecond Pulse Physics*, pages 76–78, 2009.

[26] M. King, R. Wilson, E. F. J. Bacon, E. J. Dolier, T. P. Frazer, J. Goodman, R. J. Gray, and P. McKenna. “Perspectives on laser-plasma physics in the relativistic transparency regime. ”. *Eur. Phys. J. A*, **59**:132, 2023. DOI: https://doi.org/10.1140/epja/s10050-023-01043-2.

[27] V. Bagnoud, J. Hornung, T. Schlegel, B. Zielbauer, C. Brabetz, M. Roth, P. Hilz, M. Haug, J. Schreiber, and F. Wagner. “Studying the dynamics of relativistic laser-plasma interaction on thin foils by means of Fourier-transform spectral interferometry. ”. *Phys. Rev. Lett.*, **118**:255003, 2017. DOI: https://doi.org/10.1103/PhysRevLett.118.255003.

[28] F. Böhle, M. Thévenet, M. Bocoum, A. Vernier, S. Haessler, and R. Lopez-Martens. “Generation of XUV spectral continua from relativistic plasma mirrors driven in the near-single-cycle limit.”. *J. Phys. Photonics*, **2**:034010, 2020. DOI: https://doi.org/10.1088/2515-7647/ab9715.

[29] H. Kallala, F. Quéré, and H. Vincenti. “Techniques to generate intense isolated attosecond pulses from relativistic plasma mirrors. ”. *Phys. Rev. Research*, **2**:043007, 2020. DOI: https://doi.org/10.1103/PhysRevResearch.2.043007.

[30] D. Golovin, A. Yogo, T. Pikuz, A. Faenov, H. Nishimura, M. Alkhimova, I. Skobelev, S. Pikuz, Y. Abe, and Y. Arikawa. “Development of laser driven kilo-Tesla magnetic field generator in micron scale. ”. *12th International Conference on High Energy Density Laboratory Astrophysics (HEDLA), Kurashiki, Okayama, Japan: Institute of Laser Engineering, Osaka University*, 2018.

[31] F. Wan, C. Lv, K. Xue, Z.-K. Dou, Q. Zhao, M. Ababekri, W.-Q. Wei, Z.-P. Li, Y.-T. Zhao, and J.-X. Li. “Simulations of spin/polarization-resolved laser–plasma interactions in the nonlinear QED regime.”. *Matter and Radiation at Extremes*, **8**:064002, 2023. DOI: https://doi.org/10.1063/5.0163929.

[32] L. Fedeli, A. Formenti, L. Cialfi, A. Pazzaglia, and M. Passoni. “Ultra-intense laser interaction with nanostructured near-critical plasmas.”. *Sci Rep.*, **8**: 3834, 2018. DOI: https://doi.org/10.1038/s41598-018-22147-6.

[33] S. Kubodera et al. “High-order harmonic generation in laser-produced ions. ”. *Physical Review A*, **48**:4576, 1993.

[34] H. K. Malik, S. Kumar, and Y. Nishida. “Electron acceleration by laser produced wake field: Pulse shape effect. ”. *Optics communications*, **280**:417–423, 2007. DOI: https://doi.org/10.1016/j.optcom.2007.08.013.

[35] Y. Heydarzadeh and H. Akou. “Effect of laser polarization mode on wake wave excitation in magnetized plasma. ”. *IEEE Trans. Plasma Sci.*, **48**:3088–3097, 2020. DOI: https://doi.org/10.1109/TPS.2020.3014699.

[36] P. Tomassini, V. Horny, and D. Doria. “Attosecond pulses from ionization injection wakefield accelerators. ”. *Instruments*, **7**:34, 2023.

[37] X. Wang, G. Hu, B. Shen, H. Tang, Z. Zhang, and Y. Gu. “Correlation of fast electron ejections, terahertz waves, and harmonics emitted from plasma mirrors driven by sub-relativistic ultrashort laser pulse. ”. *AIP Advances*, **12**, 2022. DOI: https://doi.org/10.1063/5.0077354.

[38] I. Y. Elnasharty. “Study on the influence of laser pulse duration in the long nanosecond regime on the laser induced plasma spectroscopy.”. *Spectrochimica Acta Part B: Atomic Spectroscopy*, **124**:1–15, 2016. DOI: https://doi.org/10.1016/j.sab.2016.08.004.

[39] K. Gopal, D. N. Gupta, and H. Suk. “Pulse-length effect on laser wakefield acceleration of electrons by Skewed laser pulses. ”. *IEEE Transactions on Plasma Science*, **49**:1152–1158, 2021. DOI: https://doi.org/10.1109/TPS.2021.3059643.

[40] V. Sharma and V. Thakur. “Maximizing energy efficiency in laser-plasma electron acceleration through pulse length and plasma density optimization. ”. *J Opt*, **97**:1–8, 2024. DOI: https://doi.org/10.1007/s12596-024-01758-5.

[41] O. J. Allegre. “Laser beam measurement and characterization techniques.”. *Handbook of Laser Micro- and Nano-Engineering, Springer*, :1885–1925, 2021. DOI: https://doi.org/10.1007/978-3-030-63647-0-45.

[42] V. F. Kovalev and V. Yu. Bychenkov. “Analytic theory of relativistic self-focusing for a Gaussian light beam entering a plasma: Renormalization-group approach.”. *Phys. Rev. E*, **99**:043201, 2019. DOI: https://doi.org/10.1103/PhysRevE.99.043201.

[43] S. T. Mahmoud and R. P. Sharma. "Relativistic self-focusing and its effect on stimulated Raman and stimulated Brillouin scattering in laser plasma interaction. ". *Physics of Plasmas*, **8**:3419–3426, 2001. DOI: https://doi.org/10.1063/1.1377048.

[44] C. Schroeder, C. Benedetti, E. Esarey, J. van Tilborg, and W. Leemans. "Group velocity and pulse lengthening of mismatched laser pulses in plasma channels. ". *Physics of Plasmas*, **18**, 2011.

[45] H. Zhong, L. Zhang, Y. Li, and D. Fan. "Group velocity mismatch-absent nonlinear frequency conversions for mid-infrared femtosecond pulses generation. ". *Scientific Reports*, **5**:10887, 2015.

[46] B. Cros. "Laser-driven plasma wakefield: Propagation effects. ". *arXiv preprint*, page 10566, 2017.

[47] A. K. Upadhyay, S. A. Samant, and S. Krishnagopal. "Tailoring the laser pulse shape to improve the quality of the self-injected electron beam in laser wakefield acceleration. ". *Physics of Plasmas*, **20**, 2013.